

Papers published in *Hydrology and Earth System Sciences Discussions* are under open-access review for the journal *Hydrology and Earth System Sciences*

**Estimating surface  
fluxes**

W. Ma et al.

# Estimating surface fluxes over the north Tibetan Plateau area with ASTER imagery

W. Ma<sup>1</sup>, Y. Ma<sup>2,3,1</sup>, M. Li<sup>1</sup>, Z. Hu<sup>1</sup>, L. Zhong<sup>2</sup>, Z. Su<sup>5</sup>, H. Ishikawa<sup>4</sup>, and J. Wang<sup>1</sup>

<sup>1</sup>Laboratory for Climate Environment and Disasters of Western China, Cold and Arid Regions Environmental and Engineering Research Institute, Chinese Academy of Sciences, LanzhouGansu 730000, China

<sup>2</sup>Institute of Tibetan Plateau Research, Chinese Academy of Sciences, Beijing, China

<sup>3</sup>School of Geography and Remote Sensing, Beijing Normal University, Beijing, China

<sup>4</sup>Disaster Prevention Research Institute, Kyoto University, Kyoto, Japan

<sup>5</sup>International Institute for Geo-Information Science and Earth Observation, Enschede, The Netherlands

Received: 22 May 2008 – Accepted: 29 May 2008 – Published: 1 July 2008

Correspondence to: W. Ma (wqma@lzb.ac.cn)

Published by Copernicus Publications on behalf of the European Geosciences Union.

Title Page

Abstract

Introduction

Conclusions

References

Tables

Figures

◀

▶

◀

▶

Back

Close

Full Screen / Esc

Printer-friendly Version

Interactive Discussion



## Abstract

Surface fluxes are important boundary conditions for climatological modeling and Asian monsoon system. The recent availability of high-resolution, multi-band imagery from the ASTER (Advanced Space-borne Thermal Emission and Reflection radiometer) sensor has enabled us to estimate surface fluxes. ASTER covers a wide spectral region with 14 bands from the visible to the thermal infrared with high spatial, spectral and radiometric resolution. The spatial resolution varies with wavelength: 15 m in the visible and near-infrared (VNIR), 30 m in the short wave infrared (SWIR), and 90 m in the thermal infrared (TIR). A parameterization method based on ASTER data and field observations has been proposed and tested for deriving surface albedo, surface temperature, Normalized Difference Vegetation Index (NDVI), Modified Soil Adjusted Vegetation Index (MSAVI), vegetation coverage, Leaf Area Index (LAI), net radiation flux, soil heat flux, sensible heat flux and latent heat flux over heterogeneous land surface in this paper. As a case study, the methodology was applied to the experimental area of the Coordinated Enhanced Observing Period (CEOP) Asia-Australia Monsoon Project (CAMP) on the Tibetan Plateau (CAMP/Tibet), which located at the north Tibetan Plateau. The ASTER data of 24 July 2001, 29 November 2001 and 12 March 2002 was used in this paper for the case of summer, winter and spring. To validate the proposed methodology, the ground-measured surface variables (surface albedo and surface temperature) and land surface heat fluxes (net radiation flux, soil heat flux, sensible heat flux and latent heat flux) were compared to the ASTER derived values. The results show that the derived surface variables and land surface heat fluxes in three different months over the study area are in good accordance with the land surface status. Also, the estimated land surface variables and land surface heat fluxes are in good accordance with ground measurements, and all their absolute percent difference (APD) is less than 10% in the validation sites. It is therefore concluded that the proposed methodology is successful for the retrieval of land surface variables and land surface heat fluxes using the ASTER data and field observation over the study

**HESSD**

5, 1705–1730, 2008

## Estimating surface fluxes

W. Ma et al.

Title Page

Abstract

Introduction

Conclusions

References

Tables

Figures

◀

▶

◀

▶

Back

Close

Full Screen / Esc

Printer-friendly Version

Interactive Discussion



area.

## 1 Introduction

The energy and water cycles play an important role in the Asian Monsoon system over the Tibetan Plateau. The Tibetan Plateau contains the world's highest elevation with average elevation about 4000 m relief features. It represents an extensive mass extending from subtropical to middle latitudes and is spanning over 25 degrees of longitude. Because of its topographic character, the plateau surface absorbs a large amount of solar radiation energy (much of which is redistributed by cryospheric processes), and undergoes dramatic seasonal changes of surface heat and water fluxes (e.g., Ye and Gao, 1979; Ye, 1981; Yanai et al., 1992; Ye and Wu, 1998; Ma et al., 2002a; Ma et al., 2006; Ma and Tsukamoto, 2002). The study on the energy exchanges between the land surface and atmosphere was also of paramount importance for the CAMP/Tibet (Ma et al., 2003a; Ma et al., 2005; Ma et al., 2006). Some interesting detailed studies concerning the land surface heat fluxes have been reported (e.g., Yang et al., 2002, 2003, 2004; Ma et al., 2002a; Choi et al., 2004; Zuo et al., 2005). These researches were, however, on point-level or a local-patch-level. Since the area the information of land-surface atmosphere interaction is required, the aggregation of the individual results into a regional scale is necessary.

Remote sensing offers the possibility to derive regional distribution of land surface heat fluxes over heterogeneous land surface in combination with sparse field experimental stations. Remote sensing data provided by satellites are a means of obtaining consistent and frequent observations of spectral albedo and emittance of radiation at elements in a patch landscape and on a global scale (Sellers et al., 1990). The land surface variables and vegetation variables, such as surface temperature  $T_{sfc}$ , surface hemispherical albedo  $r_0$ , NDVI, MSAVI, LAI and surface thermal emissivity  $\varepsilon$  is derived directly from satellite observations (e.g., Susskind et al., 1984; Che'din et al., 1985; Tucker, 1986; Wan and Dozier, 1989; Menenti et al., 1989; Becker and Li, 1990, 1995;

## Estimating surface fluxes

W. Ma et al.

Title Page

Abstract

Introduction

Conclusions

References

Tables

Figures

◀

▶

◀

▶

Back

Close

Full Screen / Esc

Printer-friendly Version

Interactive Discussion



Watson et al., 1990; Baret and Guyot, 1997; Price, 1992; Kahle and Alley, 1992; Li and Becker, 1993; Qi et al., 1994; Norman et al., 1995; Schmugge et al., 1995; Kustas and Norman, 1997; Sobrino and Raissouni, 2000; Su, 2002; Ma et al., 2003a; Ma et al., 2003b; Oku and Ishikawa, 2004; Kato, 2005). The regional heat fluxes is determined indirectly with the aid of these land surface variables and vegetation variables (Pinker, 1990).

Studies have explored several approaches to estimate the regional distribution of surface heat fluxes in recent years. These methods require specification of the vertical temperature difference between the surface temperature and the air temperature and an exchange resistance (e.g., Kustas et al., 1989; Kustas, 1990; Wang et al., 1995; Menenti et al., 1991; Menenti and Choudhury, 1993; Bastiaanssen, 1995; Kustas and Norman, 1997; Su, 2002). However, these remote sensing retrieval methods have been performed in homogeneous moist or semiarid regions, and investigations in heterogeneous landscape of high altitudes (e.g., the Tibetan Plateau area) were rare.

NOAA/AVHRR, GMS and Landsat-7 ETM data were used to determine regional land surface heat fluxes over heterogeneous landscape of the Tibetan Plateau (Ma et al., 2003a; Ma et al., 2003b; Ma et al., 2005; Ma et al., 2006; Oku et al., 2007). However, the resolution of the NOAA/AVHRR and GMS data is about 1 km×1 km, and heterogeneity, the scale of which is less than 1 km×1 km over the Tibetan Plateau area, has been omitted. So does Landsat-7 ETM data. This research is to upscale the point or patch scale field observations of land surface variables and land surface heat fluxes to regional distribution of them with the aid of high-resolution (15 m×15 m) ASTER data and in situ data.

## Estimating surface fluxes

W. Ma et al.

Title Page

Abstract

Introduction

Conclusions

References

Tables

Figures

◀

▶

◀

▶

Back

Close

Full Screen / Esc

Printer-friendly Version

Interactive Discussion



## 2 Data and methodology

### 2.1 Data

The intensive observation period (IOP) and long-term observation of the CAMP/Tibet have been done successfully in the past seven years. A large amount of data has been collected, which is the best data set so far for the study of energy and water cycle over the Tibetan Plateau. The experimental region, about  $150 \times 250 \text{ km}^2$ , includes variety of land surfaces such as a large area of grassy marshland, some desertification grassland areas, many small rivers and several lakes (Fig. 1).

The recent availability of high-resolution, multi-band imagery from the ASTER sensor has enabled us to estimate surface fluxes. ASTER covers a wide spectral region with 14 bands from the visible to the thermal infrared with high spatial, spectral and radiometric resolution. The spatial resolution varies with wavelength: 15 m in the visible and near-infrared (VNIR,  $0.52\text{--}0.86 \mu\text{m}$ ), 30 m in the short wave infrared (SWIR,  $1.6\text{--}2.43 \mu\text{m}$ ), and 90 m in the thermal infrared (TIR,  $8.1\text{--}11.6 \mu\text{m}$ ) (Yamaguchi, 1998).

The most relevant data, collected at the CAMP/Tibet surface stations (sites) to support the parameterization of land surface heat fluxes and analysis of ASTER images in this paper, consist of surface radiation budget components, surface radiation temperature, surface albedo, vertical profiles of air temperature, humidity, wind speed and direction measured at the Atmospheric Boundary Layer (ABL) towers, Automatic Weather Stations (AWSs), radio sonde, turbulent fluxes measured by eddy correlation technique, soil heat flux, soil temperature profiles, soil moisture profiles, and the vegetation state.

### 2.2 Theory and scheme

The general concept of the methodology is shown in a diagram (Fig. 2). The surface albedo for short-wave radiation ( $r_0$ ) is retrieved from narrowband-broadband conversion by Liang (Liang, 2001). ASTER has nine bands. It is expected that so many

Title Page

Abstract

Introduction

Conclusions

References

Tables

Figures

◀

▶

◀

▶

Back

Close

Full Screen / Esc

Printer-friendly Version

Interactive Discussion



Estimating surface fluxes

W. Ma et al.

Title Page

Abstract

Introduction

Conclusions

References

Tables

Figures

◀

▶

◀

▶

Back

Close

Full Screen / Esc

Printer-friendly Version

Interactive Discussion



bands should enable us to convert narrowband to broadband albedos effectively. Liang found that the conversions are quite linear. The land surface temperature ( $T_{sfc}$ ) is derived from Hook's method (Hook, 1992). Hook evaluates land surface temperature ( $T_{sfc}$ ) technique developed to extract  $T_{sfc}$  information from multispectral thermal infrared data. The radiative transfer model MODTRAN (Berk et al., 1989) computes the downward short-wave and long-wave radiation at the surface. With these results the surface net radiation flux ( $R_n$ ) is determined. On the basis of the field observations, the soil heat flux ( $G_0$ ) is estimated from  $R_n$ . The sensible heat flux ( $H$ ) is estimated from  $T_{sfc}$ , and regional latent heat flux ( $\lambda E$ ) is derived as the residual of the energy budget theorem (Liou, 2004; MA, 2006) for land surface.

### 2.2.1 Net radiation

The regional net radiation flux is derived from

$$R_n(x, y) = K_{\downarrow}(x, y) - K_{\uparrow}(x, y) + L_{\downarrow}(x, y) - L_{\uparrow}(x, y) \quad (1)$$

$$= (1 - r_0(x, y)) \cdot K_{\downarrow}(x, y) + L_{\downarrow}(x, y) - \varepsilon_0(x, y) \sigma T_{sfc}^4(x, y)$$

where  $\varepsilon_0(x, y)$  is surface emissivity,  $K_{\downarrow}(Wm^{-2})$  represents the short-wave ( $0.3-3\mu m$ ) and  $L_{\downarrow}(Wm^{-2})$  is the long-wave ( $3-100\mu m$ ) radiation components, respectively. Surface albedo  $r_0(x, y)$  is derived from narrowband-broadband conversion method by Liang (Liang, 2001). ASTER has nine bands. It is expected that so many bands should enable us to convert narrowband to broadband albedos effectively. Liang (Liang, 2001) found that the conversions are quite linear. The resultant linear equations are collated in following.

$$r_0 = 0.484\alpha_1 + 0.335\alpha_3 - 0.324\alpha_5 + 0.551\alpha_6 + 0.305\alpha_8 - 0.367\alpha_9 - 0.0015 \quad (2)$$

where  $\alpha_i (i=1-9)$  were corresponded each ASTER band surface reflection.

The incoming short-wave radiation flux  $K_{\downarrow}(x, y)(Wm^{-2})$  in Eq (1) is derived from radiative transfer model MODTRAN (Kenizys et al., 1996), The incoming long-wave radiation flux  $L_{\downarrow}(x, y) (Wm^{-2})$  in Eq. (1) is derived from MODTRAN directly as well (Ma

and Tsukamoto, 2002; Ma et al., 2006). Surface temperature  $T_{sfc}(x, y)$  (K) in Eq. (1) is derived from ASTER thermal infrared spectral radiance(Hook, 1992).

## 2.2.2 Soil heat flux

The regional soil heat flux density  $G_0(x, y)$  ( $\text{Wm}^{-2}$ ) is determined through (Choudhury, 1988)

$$G_0(x, y) = \rho_s C_s ((T_{sfc}(x, y) - T_s(x, y)) / r_{sh}(x, y)) \quad (3)$$

where  $\rho_s$  ( $\text{kgm}^{-3}$ ) is soil dry bulk density,  $C_s$  ( $\text{Jkg}^{-1}\text{K}^{-1}$ ) is soil specific heat,  $T_s(x, y)$  (K) represents soil temperature of a determined depth, and  $r_{sh}(x, y)$  ( $\text{sm}^{-1}$ ) stands for resistance of soil heat transportation. The regional soil heat flux  $G_0(x, y)$  ( $\text{Wm}^{-2}$ ) cannot directly be mapped from satellite observations through Eq. (3) for the difficulty to derive the soil heat transportation resistance  $r_{sh}(x, y)$  ( $\text{sm}^{-1}$ ) and the soil temperature at a determined depth  $T_s(x, y)$  (K) (e.g., Bastiaanssen, 1995; Ma et al., 2002b). Many investigations have shown that the midday  $G_0/Rn$  ratio,  $\Gamma$ , is reasonably predictable from special vegetation indices (Daughtry et al., 1990).  $\Gamma$  is considered as a function  $F$  which relates  $G_0/Rn$  to other variables (Ma and Tsukamoto, 2002). Some researchers have concluded that  $G_0/Rn = \Gamma = F(\text{NDVI})$  (Clothier et al., 1986; Kustas and Daughtry, 1990). A better ratio of  $G_0/Rn = \Gamma = F(r_0, T_{sfc}, \text{NDVI})$  was also found (Choudhury et al., 1987; Menenti et al., 1991; Bastiaanssen, 1995). The relationship between  $G_0(x, y)$  ( $\text{Wm}^{-2}$ ) and  $R_n(x, y)$  ( $\text{Wm}^{-2}$ ) found in the Tibetan Plateau area (Ma et al., 2003b) will be used to determine regional soil heat flux over the CAMP/Tibet area here. It means that  $G_0(x, y)$  ( $\text{Wm}^{-2}$ ) is:

$$G_0(x, y) = R_n(x, y) \cdot \frac{T_{sfc}(x, y)}{r_0(x, y)} \cdot (0.00029 + 0.00454 \bar{r}_0 + 0.00878 \bar{r}_0^2) \cdot (1 - 0.964 \text{MSAVI}(x, y)^4) \quad (4)$$

where  $\bar{r}_0$  is the average albedo.

Title Page

Abstract

Introduction

Conclusions

References

Tables

Figures

◀

▶

◀

▶

Back

Close

Full Screen / Esc

Printer-friendly Version

Interactive Discussion



### 2.2.3 Sensible heat flux

The regional distribution of sensible heat flux is calculated from

$$H(x, y) = \rho C_p \frac{T_{sfc}(x, y) - T_a(x, y)}{r_a(x, y)} \quad (5)$$

where aerodynamic resistance is

$$r_a(x, y) = \frac{1}{\kappa u_* (x, y)} \left( \ln \left( \frac{z - d_0(x, y)}{z_{0m}(x, y)} \right) + kB^{-1}(x, y) - \psi_h(x, y) \right) \quad (6)$$

where  $\kappa$  is Von-Karman constant;  $u_*$  ( $\text{ms}^{-1}$ ) is friction velocity,  $z$  (m) is reference height,  $d_0$  (m) is zero-plane displacement height,  $z_{0m}$  (m) is the aerodynamic roughness,  $kB^{-1}$  is the excess resistance for heat transportation,  $\psi_h$  is the stability correction function for heat. The friction velocity  $u_*$  is derived from

$$u_* (x, y) = \kappa u(x, y) \left( \ln \left( \frac{z - d_0(x, y)}{z_{0m}(x, y)} \right) - \psi_m(x, y) \right)^{-1} \quad (7)$$

where  $\psi_m$  is the stability correction function for momentum. From Eq. (5)–(7)

$$H(x, y) = \rho C_p \kappa^2 u(x, y) \frac{(T_{sfc}(x, y) - T_a(x, y))}{\left( \ln \frac{z - d_0(x, y)}{z_{0m}(x, y)} + kB^{-1} - \psi_h(x, y) \right) \cdot \left( \ln \frac{z - d_0(x, y)}{z_{0m}(x, y)} - \psi_m(x, y) \right)} \quad (8)$$

where  $z$  is the reference height and  $u$  is the wind speed at the reference height. In the study,  $z$  and  $u$  are determined with the aid of field measurements of AWS (Automatic Weather Stations) system at the same height.  $z_{0m}(x, y)$  in Eq. (8) over the Northern Tibetan area is calculated using Jia et al.'s model (Jia et al., 1999).  $d_0$  is the zero-plane displacement, which is calculated using Stanhill's model (Stanhill, 1969).  $T_a(x, y)$  in Eq. (8) is the regional distribution of air temperature at the reference height, it is derived from a linear method (Ma, 2007):

$$T_a(x, y) = 0.7784T_{sfc}(x, y) + 60.1706 \quad (9)$$

Title Page

Abstract

Introduction

Conclusions

References

Tables

Figures

◀

▶

◀

▶

Back

Close

Full Screen / Esc

Printer-friendly Version

Interactive Discussion



Values of the excess resistance to heat transfer,  $kB^{-1}$  versus  $u(T_{sf_c} - T_a)$  over the Northern Tibetan Plateau is following equation, (Ma, 2006)

$$kB^{-1} = 0.062u(T_{sf_c} - T_a) + 0.599 \quad (10)$$

$\psi_h(x, y)$  and  $\psi_m(x, y)$  in Eq. (8) are the integrated stability functions. For an unstable condition, the integrated stability functions  $\psi_h(x, y)$  and  $\psi_m(x, y)$  is written as (Paulson, 1970)

$$\begin{cases} \psi_m(x, y) = 2 \ln\left(\frac{1+X}{2}\right) + \ln\left(\frac{1+X^2}{2}\right) - 2 \arctan(X) + 0.5\pi \\ \psi_h(x, y) = 2 \ln\left(\frac{1+X^2}{2}\right) \end{cases} \quad (11)$$

Where  $X = \{1 - 16 \times (z - d_0(x, y)) / L(x, y)\}^{0.25}$ . For a stable condition, the integrated stability function  $\psi_h(x, y)$  and  $\psi_m(x, y)$  become (Webb, 1970)

$$\psi_m(x, y) = \psi_h(x, y) = -5 \cdot \frac{z - d_0(x, y)}{L(x, y)} \quad (12)$$

The stability function  $(z - d_0(x, y)) / L(x, y)$  is calculated by Businger's method (Businger, 1988):

$$\begin{cases} \frac{z - d_0(x, y)}{L(x, y)} = R_i(x, y) \quad (\text{unstable}) \\ \frac{z - d_0(x, y)}{L(x, y)} = R_i(x, y) / (1 - 5.2R_i(x, y)) \quad (\text{stable}) \end{cases} \quad (13)$$

where  $R_i(x, y)$  is the Richardson number; and according to the definition of the Richardson number, the approximate analytical solutions of  $R_i$  found by Yang (Yang, 2001) will be used here.

#### 2.2.4 Latent heat flux

The regional latent heat flux  $\lambda E(x, y)$  ( $\text{Wm}^{-2}$ ) is derived as the residual of the energy budget theorem (Ma, 2006) for land surface based on the condition of zero horizontal advection at  $z < z_{\text{sur}}$ , i.e.,

$$\lambda E(x, y) = R_n(x, y) - H(x, y) - G_0(x, y) \quad (14)$$

Title Page

Abstract

Introduction

Conclusions

References

Tables

Figures

◀

▶

◀

▶

Back

Close

Full Screen / Esc

Printer-friendly Version

Interactive Discussion



### 3 Case Studies and Validation

As a case study, 3 scenes of ASTER data over Tibetan Plateau are used (see Table 1). Figure 3 shows the distribution maps of surface albedo and surface temperature around the CAMP/Tibet area. Their frequency distributions are shown in Fig. 4.

Figure 5 shows the distribution maps of surface heat fluxes around the CAMP/Tibet area. Their frequency distributions are shown in Fig. 6. Figures 3 and 5 are based on 4980×4200 pixels of the ASTER data. The derived land surface heat fluxes are validated by using field measurements. The land surface variables (surface albedo and surface temperature) and land surface heat fluxes (net radiation flux, soil heat flux, sensible heat flux and latent heat flux) derived from satellite data were compared with the field measurements at BJ site. The measured surface soil heat fluxes were calculated from soil heat flux measured at -10 cm and the soil temperature measured at surface and -10 cm. The absolute percent difference (APD) can quantitatively measure the difference between the derived results ( $H_{\text{derived}(i)}$ ) and measured values ( $H_{\text{measured}(i)}$ ) as

$$\text{APD} = \frac{|H_{\text{derived}(i)} - H_{\text{measured}(i)}|}{H_{\text{measured}(i)}} \quad (15)$$

The results show the following:

1. The derived surface variables (land surface albedo and surface temperature) and surface heat fluxes (net radiation flux  $R_n$ , soil heat flux  $G_0$ , sensible heat flux  $H$  and latent heat flux  $\lambda E$ ) in three different months over the study area are in good accordance with the land surface status. The experimental area includes variety of land surfaces such as a large area of grassy marshland, some desertification grassland areas, many small rivers and several lakes; therefore these derived parameters show a wide range due to the strong contrast of surface features. Surface albedo is from 0.01 to 0.34 in July and from 0.08 to 0.55 in March and November. Surface temperature ranged from 0°C to 51.65°C in July and

Title Page

Abstract

Introduction

Conclusions

References

Tables

Figures

◀

▶

◀

▶

Back

Close

Full Screen / Esc

Printer-friendly Version

Interactive Discussion



## Estimating surface fluxes

W. Ma et al.

Title Page

Abstract

Introduction

Conclusions

References

Tables

Figures

◀

▶

◀

▶

Back

Close

Full Screen / Esc

Printer-friendly Version

Interactive Discussion



from  $-10.3^{\circ}\text{C}$  to  $36.8^{\circ}\text{C}$  in March and November. Net radiation flux changed from  $570\text{Wm}^{-2}$  to  $830\text{Wm}^{-2}$  in July and from  $80\text{Wm}^{-2}$  to  $655\text{Wm}^{-2}$  in March and November. Soil heat flux varied from  $100\text{Wm}^{-2}$  to  $220\text{Wm}^{-2}$  in July and from  $0\text{Wm}^{-2}$  to  $180\text{Wm}^{-2}$  in March and November. Sensible heat flux is from  $0\text{Wm}^{-2}$  to  $540\text{Wm}^{-2}$  in July and from  $0\text{Wm}^{-2}$  to  $520\text{Wm}^{-2}$  in March and November, and latent heat flux varied from  $0\text{Wm}^{-2}$  to  $736\text{Wm}^{-2}$  in July and  $0\text{Wm}^{-2}$  to  $288\text{Wm}^{-2}$  in March and November (see Figs. 3 and 5). Surface albedo, surface temperature and sensible heat flux around the lake in the distribution maps are much higher in July, and at the same time, net radiation flux, soil heat flux and latent heat flux are lower in the area. The reason is that most of around lake area is the desertification grass land, and it was dry and has low moisture.

2. The derived pixel value (Figs. 3 and 5) and average value (see Fig. 4 and 6) of surface temperature, net radiation flux, soil heat flux and latent heat flux in July are higher than that in March and November. It means that there is much more evaporation in summer than in winter in the north Tibetan Plateau area. It is also pointed out that the heating density ( $H+\lambda E=R_n-G_0$ ) in summer is much higher than that in winter in the central Tibetan Plateau area. The reason is that most the land surface is covered by green grass in summer and it is covered by snow and ice during winter on the experimental area.
3. The derived net radiation flux over the study area is very close to the field measurement with APD less than 3.1% (Table 2). It is caused by the improvement on surface albedo and surface temperature.
4. The regional soil heat flux derived from the relationship between soil heat flux and net radiation flux is suitable for heterogeneous land surface of the CAMP/Tibet area, and the APD is less than 9.8% at validation sites (Table 2). As a result of the relationship itself was derived from the same area (Ma et al., 2002b).
5. The derived regional sensible heat flux and latent heat flux with APD less than

Estimating surface fluxes

W. Ma et al.

Title Page

Abstract

Introduction

Conclusions

References

Tables

Figures

◀

▶

◀

▶

Back

Close

Full Screen / Esc

Printer-friendly Version

Interactive Discussion



9.8% at validation sites in the CAMP/Tibet area is in good agreement with field measurements (Table 2). The reason is that the process of atmospheric boundary layer was considered in more detail in our methodology. It is pointed that the proposed parameterization methodology for sensible heat flux and latent heat flux is reasonable, and it is used over the north Tibetan Plateau area.

4 Concluding remarks

In this study, the regional distributions of land surface variables (surface albedo and surface temperature), vegetation variables (NDVI, MSAVI, vegetation coverage and LAI) and land surface heat fluxes (net radiation flux, soil heat flux, sensible heat flux and latent heat flux) over heterogeneous north Tibetan Plateau area were derived with the aid of ASTER data and the field observation. Reasonable results of land surface variables, vegetation variables and land surface fluxes were gained in this study.

Derived the regional land surface heat fluxes over heterogeneous landscape is not an easy task. The parameterization method presented in this study is still in developing stage:

1. Only three ASTER images at a specific time of specific day are used in this study. To obtain more accurate regional land surface fluxes, their seasonal variations and even variation day by day over the CAMP/Tibet area, and even the whole Tibetan Plateau area, more field observations (ABL tower and radiation measurement system, radiosonde system, turbulent fluxes measured by eddy correlation technique, soil moisture and soil temperature measurement system etc.) and another satellite such as MODIS (Moderate Resolution Imaging Spectroradiometer) and NOAA (National Oceanic and Atmospheric Administration)/AVHRR (Advanced Very High Resolution Radiometer) have to be used. It is also worth trying SEBI (Surface Energy Balance Index; Menenti and Choudhury, 1993) method and SEBS (Surface Energy Balance System; Su, 2002).

## Estimating surface fluxes

W. Ma et al.

Title Page

Abstract

Introduction

Conclusions

References

Tables

Figures

◀

▶

◀

▶

Back

Close

Full Screen / Esc

Printer-friendly Version

Interactive Discussion



2. This study implies the parameterization method is only applicable to clear-sky days (to apply MODTRAN and detect surface temperature). In order to extend its applicability to cloudy skies, we should consider using microwave remote sensing to derive surface temperature and other land surface variables.

5 Vegetation variables cannot be validated in this study because there were no such measurements during the experiments. More attention should be paid to the measurements of vegetation variables in the coming experiments.

*Acknowledgements.* This work was under the auspices of the National Natural Science Foundation of China (40705004 and 40675012), Chinese National Key Programme for Developing Basic Sciences (2005CB422003), the Opening Foundation of Institute of Plateau Meteorology, CMA(LPM2007014), Opening Foundation of State Key Laboratory of Cryospheric Science(SKLCS 07-01) and The Key Projects of International Cooperation, Chinese Academy of Sciences(GJHZ0735). The authors also thank all the participations from China, Japan and Korea for their very hard field work during the CAMP/Tibet.

## 15 References

Baret, F. and Guyot, G.: Potentials and limits of vegetation indices for LAI and APAR assessment, *Remote Sens. Environ.*, 35, 161–173, 1997.

Bastiaanssen, W. G. M.: Ph.D. thesis, Regionalization of Surface Flux Densities and Moisture Indicators in Composite Terrain, Wageningen Agric. Univ., Netherlands, 143–161, 1995.

20 Bastiaanssen W. G. M.: PhD Thesis, Regionalization of surface fluxes and moisture indicators in composite terrain, Wageningen Agricultural University, Netherlands, 273 pp., 1995.

Becker, F. and Li, Z.-L.: Towards a local split window method over land surfaces, *Int. J. Remote Sens.*, 11, 369–393, 1990.

Becker, F. and Li, Z.-L.: Surface temperature and emissivity at various scales: Definition, measurement and related problems, *Remote Sens. Rev.*, 12, 225–253, 1995.

25 Berk, A., Bernstein, L. S., and Robertson, D. C.: MODTRAN: A moderate resolution model for LOTRAN-7, GL-TR-89-0122, Geophys. Lab., Hanscom Air Force Base, Mass, 1989.

Che'din, A., Scott, N. A., Wahiche, C., and Moulinier, P.: The improved initialisation inversion method: A high resolution physical method for temperature retrievals from Tiros-N series, *J. Clim. Appl. Meteorol.*, 24, 124–143, 1985.

Choi, T., Hong, J., Kim, J., Lee, H., Asanuma, J., Ishikawa, H., Tsukamoto, O., Gao, Z., Ma, Y., Ueno, K., Wang, J., Koike, T., and Yasunari, T.: Turbulent exchange of heat, water vapor, and momentum over a Tibetan prairie by eddy covariance and flux variance measurements, *J. Geophys. Res.*, 109, D21106, doi:10.1029/2004JD004767, 2004.

Choudhury, B. J. and Monteith, J. L.: A four-layer model for the heat budget of homogeneous land surfaces, *Q. J. R. Meteorol. Soc.*, 114, 373–398, 1988.

Choudhury, B. J., Idso, S. B., and Reginato, R. J.: Analysis of an empirical model for soil heat flux under a growing wheat crop for estimating evaporation by infrared-temperature based energy balance equation, *Agric. For. Meteorol.*, 39, 283–297, 1987.

Clothier, B. E., Clawson, K. L., Pinter, P. J., Moran, M. S., Reginato, R. J., and Jackson, R. D.: Estimating of soil heat flux from net radiation during the growth of alfalfa, *Agric. For. Meteorol.*, 37, 319–329, 1986.

Daughtry, C. S. T., Kustas, W. P., Moran, M. S., Pinter, P. J., Jackson, R. D., Brown, P. W., Nichols, W. D., and Gay, L. W.: Spectral estimates of net radiation and soil heat flux, *Remote Sens. Environ.*, 32, 111–124, 1990.

Hook, S. J., Gabell, A. R., Green, A. A., and Kealy, P. S.: A comparison of techniques for extracting emissivity information from thermal infrared data for geologic studies, *Remote Sensing of Environment*, 42, 123–135. 1992.

Jia, L., Menenti, M., and Wang, J.: Estimation of area roughness length for momentum using remote sensing data and measurements in field, *Chinese Journal of Atmospheric Sciences*, 23, 632–640, 1999, (in Chinese with English abstract).

Kahle, A. B. and Alley, R. E.: Separation of temperature and emittance in remotely sensed radiance measurements, *Remote Sens. Environ.*, 42, 107–112. 1992.

Kenizys, F. X., Abreu, L. W., Anderson, G. P., Chetwynd, J. H., Shettle, E. P., and Berk, L. S.: The MODTRAN3/2 report and LODTRAN 7 model, Phillips Lab., Geophys. Dir., Hanscom Air Force Base, Mass. Koepke, P., K. T. 1996.

Kriebel, K. T. and Dietrich, B.: The effect of surface reflection and of atmospheric parameters on the short wave radiation budget, *Adv. Space Res.*, 5, 353–354. 1985.

Kustas, W. P., Choudhury, B. J., Moran, M. S., Reginato, R. J., Jackson, R. D., Gay, L. W., and Weaver, H. L.: Determination of sensible heat flux over sparse canopy using thermal infrared

## Estimating surface fluxes

W. Ma et al.

Title Page

Abstract

Introduction

Conclusions

References

Tables

Figures

◀

▶

◀

▶

Back

Close

Full Screen / Esc

Printer-friendly Version

Interactive Discussion



## Estimating surface fluxes

W. Ma et al.

Title Page

Abstract

Introduction

Conclusions

References

Tables

Figures

◀

▶

◀

▶

Back

Close

Full Screen / Esc

Printer-friendly Version

Interactive Discussion



data, *Agric. For. Meteorol.*, 44, 197–216, 1989.

Kustas, W. P.: Estimates of evapotranspiration with a one- and twolayer model of heat transfer over partial canopy cover, *J. Appl. Meteorol.*, 29, 704–715, 1990.

Kustas, W. P., and Daughtry, C. S. T.: Estimation of the soil heat flux/net radiation ratio from spectral data, *Agric. For. Meteorol.*, 39, 205–223, 1990

Kustas, W. P. and Norman, J. M.: A two-source approach for estimating turbulent fluxes using multiple angle thermal infrared observations, *Water Resour. Res.*, 33, 1495–1508, 1997.

Li, Z.-L. and Becker, F.: Feasibility of land surface temperature and emissivity determination from AVHRR data, *Remote Sens. Environ.*, 43, 67–85, 1993.

Liang, S.: Narrowband to broadband conversions of land surface albedo I Algorithms. *Remote Sensing of Environment*, 76, 213–238, 2000.

Liou, K. N.: An introduction to atmospheric radiation(Second Edition), China Meteorol. Press, China, 2004.

Ma, W.: PhD Thesis, Estimating regional heat surface fluxes over heterogeneous landscapes of the Tibetan Plateau by using ASTER data, Chinese Academy of Sciences, China, 2007.

Ma, Y. and Tsukamoto, O.: Combining Satellite Remote Sensing With Field Observations for Land Surface Heat Fluxes Over Inhomogeneous Landscape, China Meteorol. Press, China, 2002.

Ma, Y., Tsukamoto, O., Wang, J., Ishikawa, H., and Tamagawa, I.: Analysis of aerodynamic and thermodynamic parameters over the grassy marshland surface of Tibetan Plateau, *Prog. Nat. Sci.*, 12, 36–40, 2002a.

Ma, Y., Su, Z., Li, Z.-L., Koike, T., and Menenti, M.: Determination of regional net radiation and soil heat flux densities over heterogeneous landscape of the Tibetan Plateau, *Hydrol. Processes*, 16, 2963–2971, 2002b.

Ma, Y., Su, Z., Koike, T., Yao, T., Ishikawa, H., Ueno, K., and Menenti, M.: On measuring and remote sensing surface energy partitioning over the Tibetan Plateau – From GAME/Tibet to CAMP/Tibet, *Phys. Chem. Earth*, 28, 63–74, 2003a.

Ma, Y., Ishikawa, H., Tsukamoto, O., Menenti, M., Su, Z., Yao, T., Koike, T., and Yasunari, T.: Regionalization of surface fluxes over heterogeneous landscape of the Tibetan Plateau by using satellite remote sensing, *J. Meteorol. Soc. Jpn.*, 81, 277–293, 2003b.

Ma, Y., Fan, S., Ishikawa, H., Tsukamoto, O., Yao, T., Koike, T., Zuo, H., Hu, Z., and Su, Z.: Diurnal and inter-monthly variation of land surface heat fluxes over the central Tibetan Plateau area, *Theor. and Appl.Climatol.*, 80, 259–273, 2005.

## Estimating surface fluxes

W. Ma et al.

Title Page

Abstract

Introduction

Conclusions

References

Tables

Figures

◀

▶

◀

▶

Back

Close

Full Screen / Esc

Printer-friendly Version

Interactive Discussion



- Ma, Y., Zhong, L., Su, Z., Ishikawa, H., Menenti, M., and Koike, T.: Determination of regional distributions and seasonal variations of land surface heat fluxes from Landsat-7 Enhanced Thematic Mapper data over the central Tibetan Plateau area, *J. Geophys. Res.*, 111, D10305, doi:10.1029/2005JD006742, 2006.
- 5 Ma, Y.: PhD Thesis, Determination of regional surface heat fluxes over heterogeneous landscapes by integrating satellite remote sensing with boundary layer observations, Wageningen University, 2006.
- Menenti, M., Bastiaanssen, W. G. M., and Van Eick, D.: Determination of hemispheric albedo with Thematic Mapper data, *Remote Sens. Environ.*, 28, 327–337, 1989.
- 10 Menenti, M., Bastiaanssen, W. G. M., Hefny, K., and Abd El Karim, M. H.: Mapping of ground water losses by evaporation in the Western Desert of Egypt, Rep., 1–116 pp., DLO Winand Staring Cent., Wageningen, Netherlands. 1991.
- Menenti, M. and Choudhury, B. J.: Parameterization of land surface evaporation by means of location dependent potential evaporation and surface temperature range, in *Exchange Processes at the Land Surface for a Range of Space and Time Scales*, edited by: Bolle, H. J., Feddes, R. A., and Kalma, J. D., IAHS Publ., 561–568, 1993.
- Norman, J. M., Kustas, W. P., and Humes, K. S.: A two-source approach for estimating soil and Vegetation energy fluxes from observations of directional radiometric surface temperature, *Agric. For. Meteorol.*, 77, 263–293, 1995.
- 20 Paulson, C. A.: The mathematic representation of wind speed and temperature profiles in the unstable atmospheric surface layer, *J. Appl. Meteorol.*, 9, 856–861. 1970.
- Pinker, R. T.: Satellites and our understanding of the surface energy balance, *Paleogr. Palaeoclimatol. Palaeoecol.*, 82, 321–342. 1990.
- Price, J. C.: Estimating vegetation amount from visible and near infrared albedo, *Remote Sens. Environ.*, 41, 29–34, 1992.
- 25 Qi, J., Chehbouni, A., Huete, A. R., Kerr, Y. H., and Sorooshian, S.: A modified soil adjusted vegetation index, *Remote Sens. Environ.*, 48, 119–126. 1994.
- Kato, S. and Yamaguchi, Y.: Analysis of urban heat-island effect using ASTER and ETM+ Data: Separation of anthropogenic heat discharge and natural heat radiation from sensible heat flux, *Remote Sensing of Environment*, 99, 44–54. 2005.
- 30 Schmutge, T. J., Hook, S., and Kahle, A.: TIMS observation of surface emissivity in HAPEX-Sahel, paper presented at International Geoscience and Remote Sensing Symposium, Inst. of Electr. and Electron.Eng., Florence, Italy, 1995.

## Estimating surface fluxes

W. Ma et al.

Title Page

Abstract

Introduction

Conclusions

References

Tables

Figures

◀

▶

◀

▶

Back

Close

Full Screen / Esc

Printer-friendly Version

Interactive Discussion



- Sellers, P. J., Rasool, S. I., and Bolle, H. J.: A review of satellite data algorithms for studies of the land surface, *Bull. Am. Meteorol. Soc.*, 71, 1429–1447, 1990.
- Shunlin Liang.: Narrowband to broadband conversions of land surface albedo, *Remote Sensing of Environment*, 76, 213–238, 2001.
- 5 Sobrino, J. A. and Raissouni, N.: Toward remote sensing methods for land cover dynamic monitoring: application to Morocco, *International Journal of Remote Sensing*, 21, 353–366, 2000.
- Stanhill, G.: A simple instrument for the ground measurement of turbulent diffusion flux *Journal of Applied Meteorology*, 8, 509–513, 1969.
- 10 Su, Z.: The Surface Energy Balance System (SEBS) for estimation of turbulent heat fluxes, *Hydrol. Earth Syst. Sci.*, 6, 85–99, 2002, <http://www.hydrol-earth-syst-sci.net/6/85/2002/>.
- Susskind, J., Rosenfield, J., Renter, D., and Chahine, M. T.: Remote sensing of weather and climate parameters from HIRS2/MSU on TIROS-N, *J. Geophys. Res.*, 89, 4677–4697, 1984.
- 15 Tucker, C. J.: Monitoring the grasslands of semi-arid Africa using NOAA AVHRR data, *Int. J. Remote Sens.*, 7–11, 1383–1622, 1986.
- Wan, Z. and Dozier, J.: Land surface temperature measurement from space: Physical principles and inverse modelling, *IEEE Trans. Geosci. Remote Sens.*, 27, 268–278, 1989.
- Wang, J., Ma, Y., Menenti, M., Bastiaanssen, W. G. M., and Mistsuta, Y.: The scaling-up of processes in the heterogeneous landscape of HEIFE with the aid of satellite remote sensing, *J. Meteorol. Soc. Jpn.*, 73, 1235–1244, 1995.
- 20 Watson, K., Kruse, F., and Hummer-Miler, S.: Thermal infrared exploration in the Carlin trend, *Geophysics*, 55, 70–79. 1990.
- Y. Oku and Ishikawa, H.: Estimation of Land Surface Temperature over the Tibetan Plateau Using GMS Data, *J. Appl. Meteorol.*, 43, 548–561. 2004.
- 25 Y. Oku, Ishikawa, H., and Su, Z.: Estimation of Land Surface Energy Fluxes over the Tibetan Plateau using GMS Data, *J. Appl. Meteorol. Climatol.*, 46, 183–195. 2007.
- Y. Yamaguchi, Kahle, A. B., Tsu, H., Kawakami, T., and Pniel, M.: Overview of the Advanced Spaceborne Thermal Emission and Reflection Radiometer (ASTER), *Trans. Geosci. Remote Sens.*, 36, 1062–1071, 1998.
- 30 Yanai, M., Li, C., and Song, Z.: Seasonal heating of the Tibetan Plateau and its effects on the evolution of the Asian summer monsoon, *J. Meteorol. Soc. Jpn.*, 70, 319–351, 1992.
- Yang K., Tamai, N., and Koike, T.: Analytical solution of surface layer similarity equations, *J.*

- Appl. Meteorol., 40, 1647–1653, 2001.
- Yang, K., Koike, T., Fujii, H., Tamagawa, K., and Hirose, N.: Improvement of surface flux parameterizations with a turbulence-related length, Q. J. R. Meteorol. Soc., 128B, 2073–2088. 2002.
- 5 Yang, K., Koike, T., and Yang, D.: Surface flux parameterization in the Tibetan Plateau, Bound. Lay. Meteorol., 116, 245–262. 2003.
- Yang, K., Koike, T., Ishikawa, H., and Ma, Y.: Analysis of the surface energy budget at a site of GAME/Tibet using a single-source model, J. Meteorol. Soc. Jpn., 82, 131–153. 2004.
- Ye, D. and Gao, Y.: The Meteorology of the Qinghai-Xizang (Tibet) Plateau (in Chinese), 1–278, 10 Sci. Press, China, 1979.
- Ye, D.: Some characteristics of the summer circulation over the Qinghai-Xizang (Tibet) Plateau and its neighborhood, Bull. Am. Meteorol. Soc., 62, 14–19, 1981.
- Ye, D. and Wu, G.: The role of the heat source of the Tibetan Plateau in the general circulation, Meteorol. Atmos. Phys., 67, 181–198, 1998.
- 15 Zuo, H., Hu, Y., Li, D., Lu, S., and Ma, Y.: Seasonal transition and its boundary characteristics in Amdo area of Tibetan Plateau, Prog. Nat. Sci., 15, 239–245, 2005.

## HESSD

5, 1705–1730, 2008

### Estimating surface fluxes

W. Ma et al.

Title Page

Abstract

Introduction

Conclusions

References

Tables

Figures

◀

▶

◀

▶

Back

Close

Full Screen / Esc

Printer-friendly Version

Interactive Discussion



## Estimating surface fluxes

W. Ma et al.

Title Page

Abstract

Introduction

Conclusions

References

Tables

Figures

◀

▶

◀

▶

Back

Close

Full Screen / Esc

Printer-friendly Version

Interactive Discussion



**Table 1.** The solar zenith angles information of 3 ASTER scenes.

Date	HH:MM:SS(Beijing Time)	solar zenith angle(degree)
24 Jul 2001	12:47:59	19.64792
29 Nov 2001	12:44:03	54.80759
12 Mar 2002	12:47:25	38.96375

## Estimating surface fluxes

W. Ma et al.

**Table 2.** Comparison of the derived results (RS results) versus those measured values (Observations) at the CAMP/Tibet site with APD.

Date	Items	$Rn(Wm^{-2})$	$H(Wm^{-2})$	$G_0(Wm^{-2})$	$\lambda E(Wm^{-2})$
24 Jul 2001	Observations	620.15	262.07	123.14	234.94
	RS results	637.03	268.24	133.16	243.60
	APD	2.6%	2.3%	7.5%	3.6%
29 Nov 2001	Observations	297.94	214.87	4.8	25.58
	RS results	307.40	201.22	4.69	27.20
	APD	3.1%	6.8%	2.1%	6.0%
12 Mar 2002	Observations	391.77	327.57	48.57	15.64
	RS results	387.64	350.74	53.74	17.35
	APD	1.0%	6.6%	9.6%	9.8%

Title Page

Abstract

Introduction

Conclusions

References

Tables

Figures

◀

▶

◀

▶

Back

Close

Full Screen / Esc

Printer-friendly Version

Interactive Discussion



## Estimating surface fluxes

W. Ma et al.

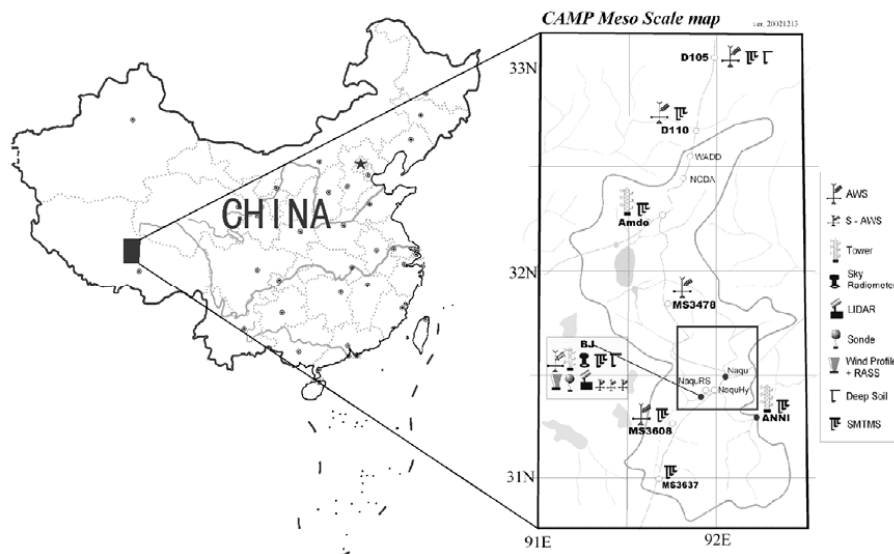


**Fig. 1.** Study area map and the sites during the CAMP/Tibet.

Title Page

Abstract

Introduction

Conclusions

References

Tables

Figures

◀

▶

◀

▶

Back

Close

Full Screen / Esc

Printer-friendly Version

Interactive Discussion



Estimating surface fluxes

W. Ma et al.

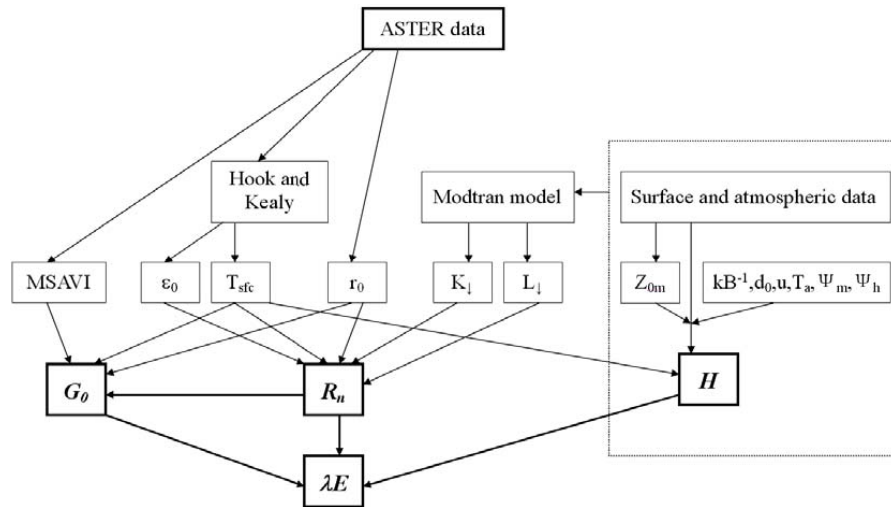


Fig. 2. Diagram of parameterization procedure by combining ASTER data with field observations.

Title Page

Abstract

Introduction

Conclusions

References

Tables

Figures

◀

▶

◀

▶

Back

Close

Full Screen / Esc

Printer-friendly Version

Interactive Discussion



## Estimating surface fluxes

W. Ma et al.

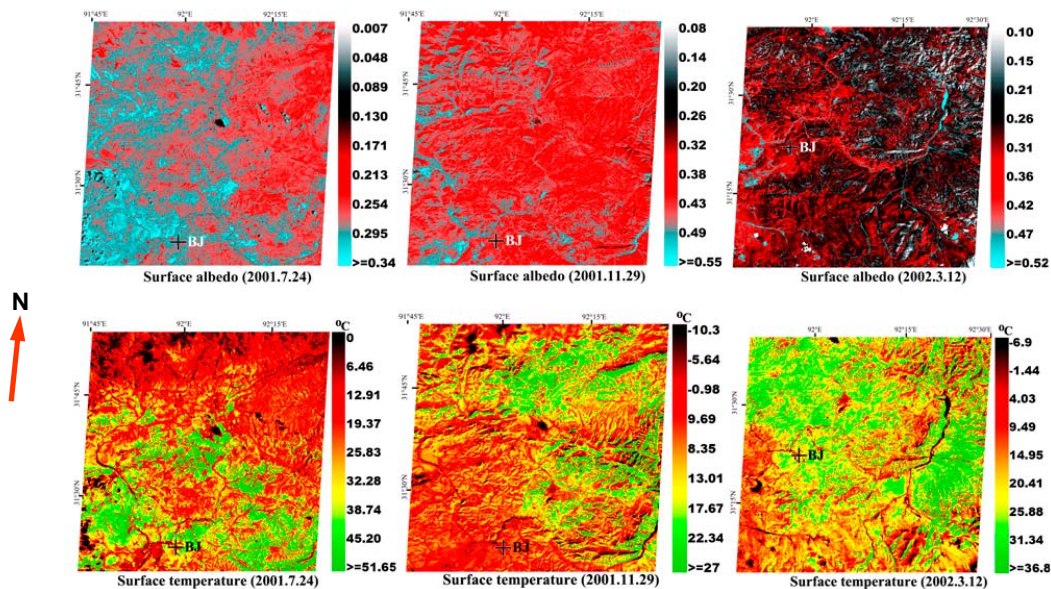


Fig. 3. Distribution maps of land surface variables over the CAMP/Tibet area.

Title Page

Abstract

Introduction

Conclusions

References

Tables

Figures

◀

▶

◀

▶

Back

Close

Full Screen / Esc

Printer-friendly Version

Interactive Discussion



## Estimating surface fluxes

W. Ma et al.

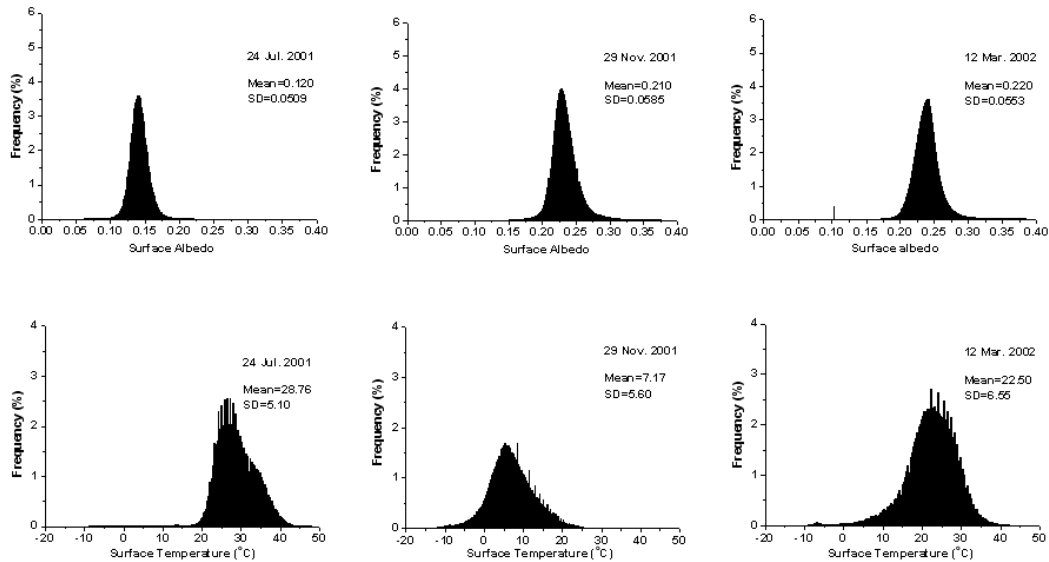


**Fig. 4.** Frequency distribution of surface albedo and surface temperature for the CAMP/Tibet area at 12:45 Beijing Time.

Title Page

Abstract

Introduction

Conclusions

References

Tables

Figures

◀

▶

◀

▶

Back

Close

Full Screen / Esc

Printer-friendly Version

Interactive Discussion



## Estimating surface fluxes

W. Ma et al.

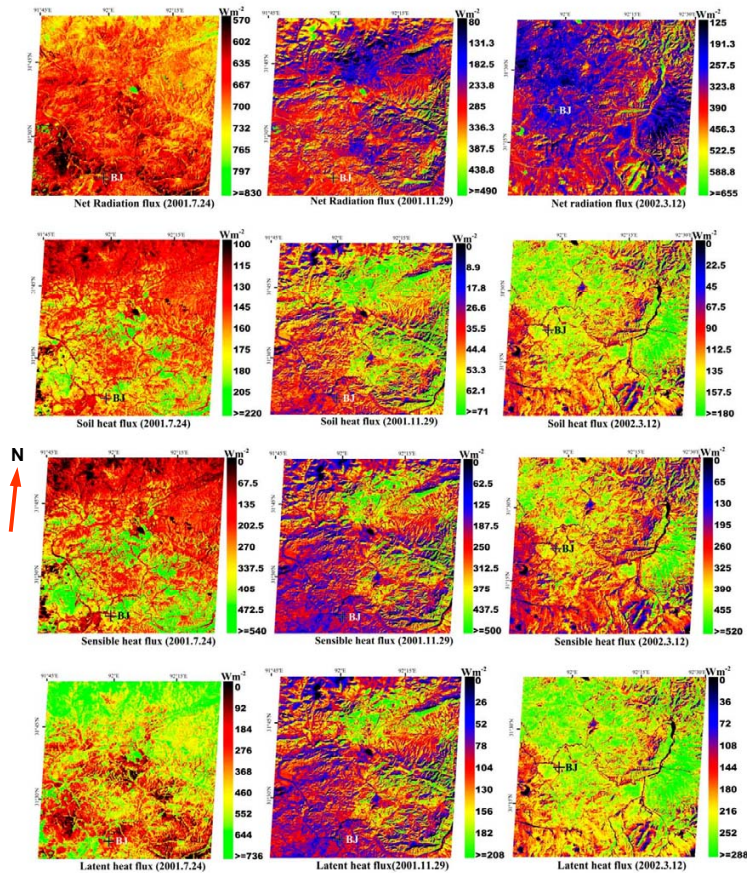


**Fig. 5.** Distribution maps of land surface heat fluxes over the CAMP/Tibet area.

Title Page

Abstract

Introduction

Conclusions

References

Tables

Figures

◀

▶

◀

▶

Back

Close

Full Screen / Esc

Printer-friendly Version

Interactive Discussion



## Estimating surface fluxes

W. Ma et al.

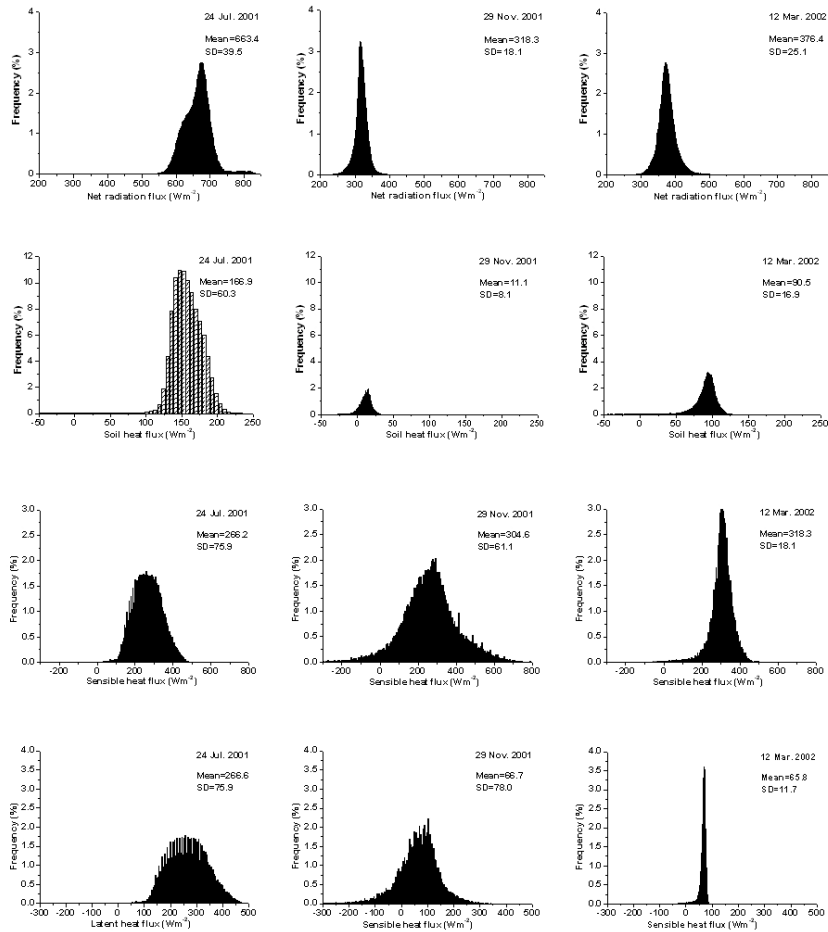


**Fig. 6.** Frequency distribution of land surface heat fluxes for the CAMP/Tibet area at 12:45 Beijing Time.

Title Page

Abstract

Introduction

Conclusions

References

Tables

Figures

◀

▶

◀

▶

Back

Close

Full Screen / Esc

Printer-friendly Version

Interactive Discussion

